

Chapter 4

GEOMORPHIC CHANNEL PATTERNS OF DELTAS VERSUS DISTAL SUBMARINE FANS: IMPLICATIONS FOR SEDIMENTATION PROCESSES ON EARTH AND MARS

Abstract

Channel systems at the distal limits of submarine fans show variability in channel size and bifurcation patterns. This information is useful in constraining channel properties in static reservoir models, e.g. the mean and range of values typical for channel dimensions, sinuosity, and branching angles. Criteria were evaluated that might help discriminate between deltas and submarine fans based on the bifurcation pattern of the channels present on the fans, i.e. by using the properties of channel width, length, sinuosity, branching angle and gradients. Submarine fans and deltas show nonlinear decreases in mean channel width and channel length with increasing bifurcation order. Sinuosity is also found to decrease down fan. Channel branching angles appear to be stochastic and do not provide a meaningful measure to discriminate between fan types. The trends of mean channel length versus mean channel width follow a power law. The steepness of the power law trend does not appear to correlate with the dominant grain size present on the fan, the water depth of the fan, margin type or drainage basin size. The exponents of the power law fit for deltas are somewhat smaller than the exponents for submarine fans, but taking into account the uncertainties on the values, the two types of fans cannot be wholly distinguished.

We also characterized the channel patterns on a Martian submarine fan and delta and compared them to terrestrial fans. Channel lengths fall off slightly more slowly for a

given decrease in channel width on Mars possibly due to a longer advection length scale on Mars due to lower gravity.

4.1 Introduction

Understanding channel bifurcation patterns is important for understanding dynamics of sediment transport systems, in addition to providing constraints for reservoir models. The channels present on submarine fans are important hydrocarbon reservoirs in many areas of the world (Deptuck et al. 2007). Submarine channels form sand-rich channel complexes and the size, lateral continuity, connectivity and heterogeneity of sand bodies are important constraints in reservoir models (Clark and Pickering 1996; Labourdette 2007). Characterizing the variability in channel size and bifurcation pattern present in channel systems at the distal limits of submarine fans can be used to constrain channel properties in static reservoir models. We compare the channel bifurcation patterns present on submarine fans and deltas on both Earth and Mars to test whether the differences in sediment transport affect the channel bifurcation pattern.

If the channel patterns on deltas and submarine fans are indistinguishable, then this might provide a short-cut to modeling deepwater systems which, by virtue of their depositional setting, provide only difficult and expensive access for study. Instead, the scaling relationships from well-characterized deltas could be applied to submarine fan exploration prospects with only minor adjustments. In contrast, if the channel patterns on submarine fans and deltas are distinct, then this observation could provide an important criterion to interpret depositional environment for fans where the water depth is unknown.

A further application, of interest to planetary science, would be to provide a basis for separation of subaerial from fully subaqueous sediment bodies on planets like Mars.

This study tested whether it is possible to discriminate between deltas and submarine fans based on the bifurcation pattern of the channels present on the fans by using the properties of channel width, length, sinuosity, branching angle and gradients. Channels on six terrestrial submarine fans, two terrestrial deltas, two Martian submarine fans and one Martian delta were compared.

4.2 Background

One might expect the channel patterns on deltas and submarine fans to differ, since channels on deltas are fed by rivers whereas channels on submarine fans are fed by turbidity currents. These turbidity currents flow down sinuous deep-water channels through laterally extensive channel-levee systems that locally aggrade significantly above the low gradient fan surface (Wynn et al. 2007). These levees can build up to hundreds of meters above the submarine fan surface, and by definition this occurs on the upper and middle submarine fan (Flood and Damuth 1987). The channels are thought to avulse frequently with only one channel active at a time (Damuth et al. 1983b; Wynn et al 2007). Levees exist for channels in the upper and middle submarine but are not seen on lower submarine fans (Flood and Damuth 1987).

Many studies have examined submarine channels on the upper and middle regions of submarine fans (Flood and Damuth 1987; Clark et al. 1992; Deptuck et al. 2007; Kolla

et al. 2007; Wynn et al. 2007), but few studies focus on channels across lower submarine fans (Twitchell et al. 1992; Nelson et al. 1992). The channels on upper and middle submarine fans are similar to river channels in several aspects of their planform geometries (Clark et al. 1992; Flood and Damuth 1987). Also similar to subaerial river channels, submarine channels show high sinuosity, abandoned meander loops, lateral channel migration, crevasse splays and abandoned terraces (Damuth et al. 1983a, Pickering et al. 1986; Karl et al. 1989; Beaufouef et al. 2002). Yet, there is a lower occurrence of meander loop cutoffs and avulsions in submarine channels as compared to subaerial channels, which may be due to stabilization of the sinuosity by deposition on both the inner and outer bends of submarine channels (Kane et al. 2008). Strongly bypassing turbidity currents deposit on the inner channel bend, whereas weakly bypassing flows deposit on the outer channel bend, a case unique to submarine channels (Kane et al. 2008). Straub et al. (2008) conducted laboratory experiments on turbidity current deposition in sinuous channels and found high deposition rates on the outer banks of bends. They concluded that sedimentation rates were highest where near-bed sediment concentration was greatest, which occurs on the outer banks of channel bends. This contrasts with subaerial river channels where bedload transport dominates the evolution of channel morphology (Dietrich and Whiting 1989). Since bedload transport does not cover the steep outer banks of bends, the sidewalls are exposed to erosion by the moving fluid (Straub et al. 2008).

Distributary channel patterns on deltas are controlled by a combination of channel mouth bifurcations and avulsions, with channel bifurcations being more common (Slingerland and Smith 2004; Edmonds and Slingerland 2007; Jerolmack and Mohrig

2007; Edmonds et al. 2009). Recent studies that focus on understanding bifurcations of channels in deltas have debated whether bifurcations are caused by the buildup of mouth bars or the deceleration of jet plumes (Wright 1977; Wellner et al. 2005; Edmonds and Slingerland 2007). As discussed by Wright (1977), a sediment-laden flow enters a standing body of water as a turbulent jet at the mouth of a distributary channel and begins to spread laterally. As the turbulent jet decelerates, its transport energy diminishes, causing deposition of material. Bed friction in the shallow depths basinward of a river mouth causes rapid deceleration, lateral expansion and sediment deposition in a mouth bar.

Distributary channel bifurcation patterns will depend on where mouth bars form as well as their final location. Edmonds and Slingerland (2007) document bifurcation patterns on several deltas, and they show that distributary channel widths and lengths decrease nonlinearly with successive bifurcation number (order). Channel width decreases with increasing bifurcation order, defined as the number of bifurcations upstream of the channel in question, because the channels are adjusting to a decreasing discharge (Edmonds and Slingerland 2007). They suggest that channel length decreases are the result of jet momentum flux decreases. Since the distance to the river mouth bar is proportional to jet momentum flux, a decreased momentum flux would lead to smaller distances between successive mouth bars and hence more closely spaced channel bifurcations. Olariu and Bhattacharya (2006) document terminal distributary channels on several river-dominated deltas and measure the channel orientations with respect to the main trunk channel. They found that these angles were related to the overall dominant processes operating on the delta (eg. wave dominated, river dominated or tide dominated deltas). Since delta-plain

gradients are small and sedimentation rates are high, the direction of distributary channels can be easily changed (Olariu and Bhattacharya 2006). With each bifurcation of the channel, the discharge is split between the newly formed channels, and hence the channels become smaller in a downstream direction.

The purpose of this study was to compare morphometric data on submarine distributary networks to delta distributary networks to see if the patterns differ enough to allow discrimination between fan types where the environment of deposition is unknown. Our mapping of the channels on the distal limits of submarine fans and fluvial deltas on both Earth and Mars shows that the bifurcation patterns on the two types of fans are indistinguishable using simple parameters.

4.3 Study Sites

Six terrestrial submarine fans, two Martian submarine fans, two terrestrial deltas and one Martian delta were examined in this study. We selected the terrestrial submarine fans based on the availability of side-scan sonar or seismic images of sufficient quality to be able to distinguish the channel patterns. Wax Lake delta, LA, was selected since it has had relatively little human influence impacting its morphology. The Lena delta, Russia, was chosen since it is in a permafrost region, and conditions on Mars when the deltas and submarine fans formed may have been similar (Baker 2006). Table 4.1 lists basic properties of each fan. The locations of the terrestrial submarine fans and deltas are shown in Figure 4.1.

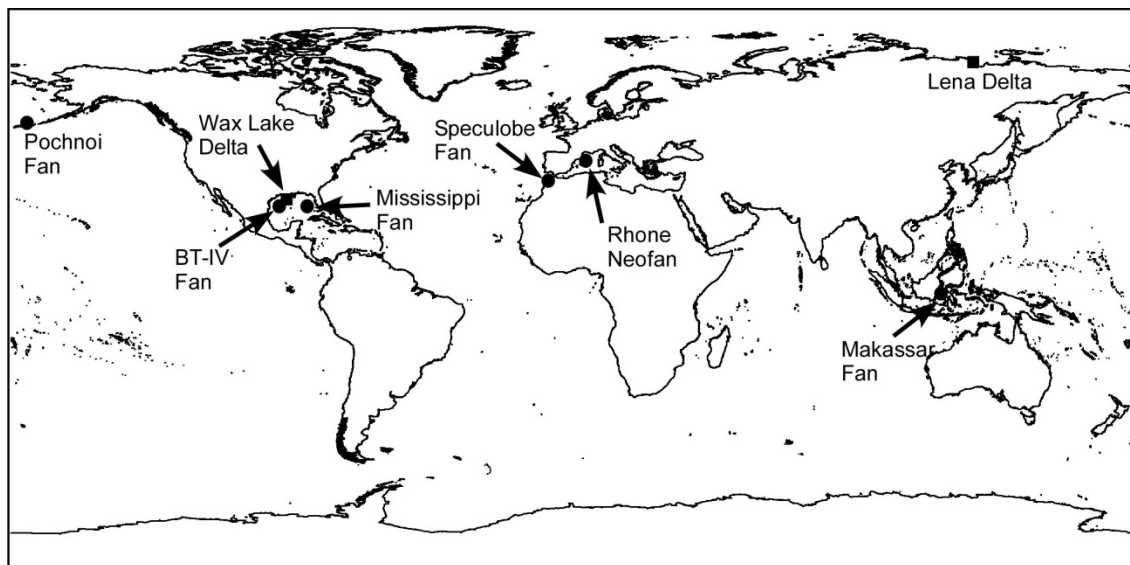


Figure 4.1 Map showing location of fans in this study. Squares represent the locations of deltas and circles represent the locations of submarine fans.

4.3.1 Submarine Fans

Speculobe

The Speculobe fan is a small (3 by 14 km) seafloor fan located in the Gulf of Cadiz offshore Spain. The fan is sand-rich and contains predominantly fine to medium grained sand and a low clay content <1.5 vol % (internal Shell data). It lies on the lower slope of the Gulf of Cadiz at a water depth of approximately 1500 m. The width of the lower slope varies from 50 km to 200 km, and this area has been tectonically active in the Quaternary (Hernandez-Molina et al. 2006).

Fan	Grain size	Water depth (m)	Fan Length (km)	Fan Width (km)	Fan Area (km ²)	Fan Volume (km ³)	Drainage Basin Area (km ²)	Tectonic State
Bering	?	?	400	190	20,000 [†]	?	1.2×10 ⁵	Active
BT Basin IV	sand	1500	16 ^c	8 ^c	128	12.8 [*]	1.2×10 ⁵	Passive
Makassar	mud	2400	65 ^a	50 ^a	2500 ^a	7.5 [‡]	7.5×10 ⁴	Active
Mississippi	mud	3200	600 ^b	500	300,000 ^b	290,000 ^b	4.76×10 ⁶	Passive
Rhone Neofan	sand	2400	100	14	1430 ^b	25 ^b	9.0×10 ⁴	Passive
Speculobe	sand	1500	14	3	48	0.3 [‡]	5.7×10 ⁴	Active ^e
Melas N	?	?	2.1	1.5	2.3 ^d	0.05 ^d	~500	-
Melas S	?	?	1.3	3	4.3 ^d	0.10 ^d	~500	-
Wax Lake Delta	sand	~0	11	12	40	0.08 ^{**}	?	Passive
Lena Delta	sand	~0	190	190	32,000	?	2.5×10 ⁶	Active
Eberswalde Delta	?	~0	13.7	11.5	102	?	4800	-

Table 4.1 Properties of the fan systems examined in this study. Grain size refers to the dominant grain size. Tectonic state refers to whether or not the area was tectonically active when the fan was deposited. †Shell cores show that the depth of the sand composing the fan near the centre is 8 m and is 2 m near the edges of the fan. An intermediate depth value of 6 m was used to calculate the volume (Shell Speculobe Report Phase II). ‡The longest core of the fan lobes described in Orange et al. (2006) is 3 m, so this value was used to calculate the volume of the fan, although the actual thickness is likely to be larger. *Calculated assuming thickness of fan is 100 m (Beaubouef et al. 2003). **Thickness of sediments ranges between 0.5-3 m (Wellner et al.2005); An intermediate value of 2 m was used for this volume calculation. a. Orange et al. 2006, b. Wynn et al. 2007, c. Beaubouef et al. 2003, d. Metz et al. 2009b, e. Hernandez-Molina et al. 2006, f. Herman et al. 1996.

Makassar Straits

The seafloor fan in Makassar Straits is a very low relief mud-rich submarine fan located between the islands of Borneo and Sulawesi. It is approximately 40 km wide by 60 km long and is located at a water depth of ~2400 m. Makassar Straits formed during the Eocene in response to crustal extension, and after Borneo was uplifted during the Neogene, the massive outbuilding of the Mahakam Delta occurred (Hall et al. 2009). Much of this deltaic sediment was redeposited as turbidites in the Makassar Basin (Jackson 2004; Konyukhov 2009). Differential uplift in the Late Pliocene changed the direction of sediment transport from eastward to westward when mini-basins associated with the long limbs of west-verging anticlines filled with coarse-grained turbidites (Jackson 2004).

Mississippi

The Mississippi submarine fan is a large (>600 km long), mud-rich seafloor fan with an area of ~300,000 km² and a volume of 290,000 km³ (Fig. 4.2A; Wynn et al 2007). This passive-margin submarine fan was sourced through a major submarine valley system at the shelf margin and upper slope, which in turn was fed by a large river (the ancestral Mississippi River) with its continental drainage system. It was largely constructed during the Plio-Pleistocene when sedimentation rates were as high as 6-11 m per 1000 years during the Pleistocene glacials (Wynn et al. 2007). Finger-shaped backscatter patterns on the edge of the fan correlated with restricted sand-silt beds suggest channelized flows may have been an important sediment-delivering process to the distal fan (Twitchell et al. 1992; Nelson et al. 1992).

Brazos-Trinity Basin IV

The Brazos-Trinity Basin IV ponded apron is located in the northwestern Gulf of Mexico and is formed in the terminal basin of four linked intraslope basins (Fig. 4.2B). The apron is of Pleistocene age (Beaubouef et al 2003), and is deposited on a relatively shallow synclinal ramp with no outlet (Mallarino et al 2006). The apron is located in ~1500 m of water depth and is 8 km wide by 16 km long with a maximum thickness of 100 m (Beaubouef et al 2003). Its oval-shaped basin is thought to be a salt withdrawal mini-basin and the main axis is oriented in a northeast-southwest direction (Mallarino et al

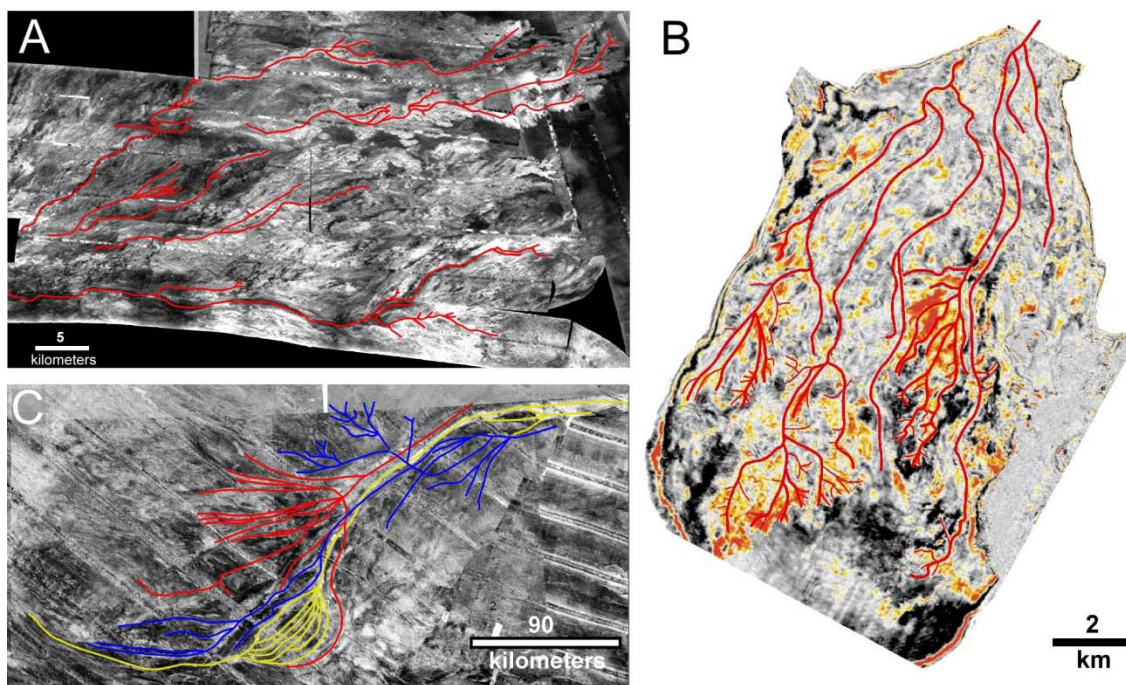


Figure 4.2 Examples of channel mapping on side-scan sonar and seismic images. A.) Side-scan sonar image of Mississippi submarine fan showing the channels mapped in red. B.) Horizon slice from 20 ms below the top of the fan extracted from a high-resolution 3D seismic volume of the Brazos-Trinity Basin IV ponded apron from Beaubouef et al. (2003). Channels are mapped in red. C.) 6.6 kHz side-scan sonar image of the Bering fan with the channels mapped in different colors which reflect the relative ages of the channels based on cross cutting relationships (yellow are oldest, blue are youngest).

2006). Sediment is supplied to the apron from an inlet channel to the northeast (Beaubouef et al 2003). Cores show the proximal fan is sand-rich while the periphery and areas further down-fan are more mud-rich (Beaubouef et al 2003; Mallarino et al 2006). The majority of the sand was deposited between 115-15 ka, with maximum accumulation rates during the Last Glacial Maximum (Mallarino et al 2006).

Rhone Neofan

The Rhone Neofan is part of the much larger Petit-Rhone Fan, formed from the most recent avulsion of the Rhone channel in the Gulf of Lion at a water depth of ~2400 m. The Gulf of Lion is a young passive margin with a high subsidence rate, and is supplied with sediments from the Rhone River (Droz et al. 2006). The continental shelf is 80 km wide, and the slope is strongly incised by canyons (Droz et al. 2006). Coring shows that the Neofan is composed of medium to fine-grained, well-sorted sand (Torres et al. 1997; Droz et al. 2001). The growth of the Neofan began at 80 ka BP and continued until 18 ka BP and is thought to have been controlled by Quaternary glacio-eustatic changes. The Rhone Neofan is up to 70 m thick, covers an area of 1430 km² and had a volume of 25 km³ (Wynn et al. 2007).

Bering Fan

The Bering fan is one of three main canyon-channel systems located in the Aleutian Basin in the Bering Sea (Fig. 4.2C; Herman et al., 1996). The area of the Bering fan is

20,000 km², and it is thought to be a very young feature, possibly of late Pliocene-Quaternary age (Herman et al., 1996).

4.3.2 Deltas

Wax Lake Delta

Wax Lake Delta is a modern bay head fan delta located at the mouth of the Wax

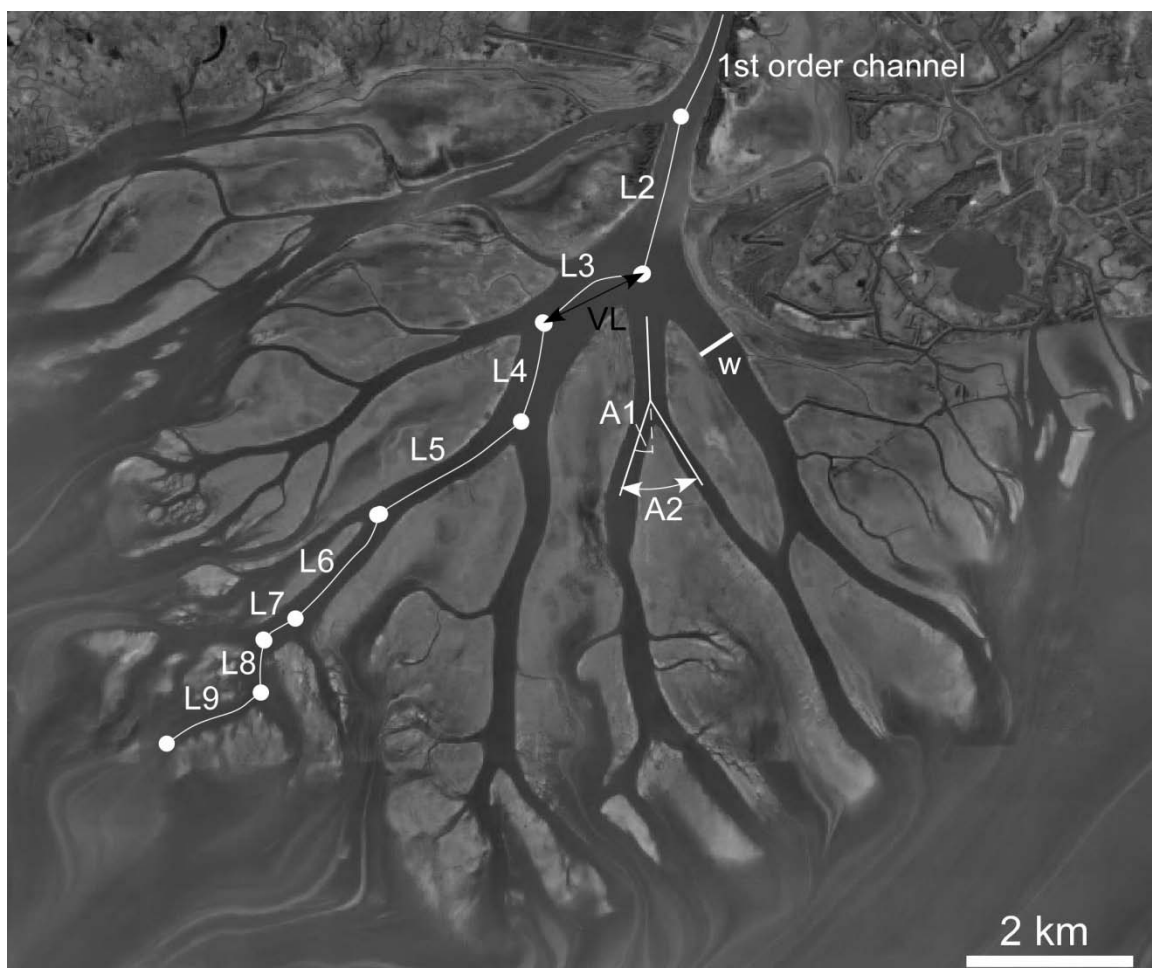


Figure 4.3. High-altitude aerial photograph of the Wax Lake Delta taken in 2002. The first order channel is noted along with bifurcation points (circles), channel lengths (L), valley lengths (VL), channel width (w), and branching angles (A1 and A2).

Lake outlet, LA, which is a man-made channel excavated in 1941 (Fig. 4.3; Wellner et al. 2005; Parker and Sequeiros 2006). Deltaic deposition at the Wax Lake Outlet was entirely subaqueous until 1972 when the tops of several deltaic sublobes were exposed at mean low tide (Wellner et al. 2005). The formation of this delta was tracked through time by images taken over the last thirty years. There have been negligible human influences on the delta since the original excavation of the channel.

Lena Delta

The Lena delta is a river-dominated delta located at the Laptev Sea coast in northeast Siberia in a permafrost region (Olariu and Bhattacharya 2006). The permafrost may affect river bank stability (Lawson 1983). The evolution of the delta has been strongly influenced by tectonic forces over the last 80,000 years (Are and Reimnitz 2000). A large fraction of the delta is underlain by Devonian bedrock which may control the channel distributary pattern (Are and Reimnitz 2000).

4.3.3 Mars Fans

Two submarine fans have been identified in southwest Melas Chasma in Valles Marineris on Mars (see Fig. 4.6). These submarine fans were identified based on their morphologic similarity to the Mississippi submarine fan complex. The Melas fans are composed of multiple channelized lobate deposits. The northern fan is 2.1 km long and has

an area of 2.3 km² while the southern fan is 1.3 km long with an area of 2.2 km² (Metz et al., 2009b).

The Eberswalde delta is located within a 65 kilometer diameter crater at 24.3° S latitude, 33.5° W longitude on Mars (Malin and Edgett 2003). The delta is an erosional remnant of a larger and thicker paleodeltaic deposit and is composed of six separate deltaic lobes (Lewis and Aharonson 2006; Wood 2006). The delta surface is covered by numerous channel forms and bifurcating distributaries that appear as present-day topographic highs after being elevated by erosion and deflation of the surrounding host sediments (Bhattacharya et al. 2005; Wood 2006).

4.4 Data

Side-scan sonar or seismic images of six terrestrial submarine fans were examined in this study along with aerial photographs and satellite images of two terrestrial deltas. Satellite images of Martian submarine fans and a delta were also examined.

4.4.1 Submarine Fans

Deep-towed 100 kHz high-resolution side-scan sonar collected by UK-TAPS during the TTR-12 cruise in 2002 of the Speculobe fan was used along with a 2 m contour interval bathymetric map compiled on the basis of this survey. A 100 kHz side-scan sonar survey of the Rhone Neofan collected by UK-TAPS was also used. We used high-resolution SeaMARC IA 27-30 kHz side-scan sonar images of the Mississippi submarine fan acquired in 1990 by the U.S. Geological Survey (Twitchell et al. 1992). 6.5 kHz Gloria

side-scan sonar images of the Bering fan acquired by the USGS between 1986-1987 were also used (EEZ-SCAN Scientific Staff 1991). We used multibeam backscatter images acquired by Unocal in 2003 to study the basin floor fan located in the Makassar Straits as well as a 10 m contour interval bathymetric map. A horizon slice from 20 ms below the top of the fan extracted from a high-resolution 3D seismic volume from Beaubouef et al. (2003) was used to study Basin IV in the Brazos-Trinity system.

Several factors can affect the backscatter pattern returned from side-scan sonar profiles including the geometry of the sensor-target system, the roughness of the seafloor, and the composition and grain size of the surface (Blondel and Murton 1997). Gardner et al. (1991) found that regional backscatter patterns correlate, at least qualitatively, with lithostratigraphy.

4.4.2 Deltas

The Wax Lake Delta was studied by using a high-altitude infrared aerial photograph (pixel size ~16 m) taken in 2002 at low tide and a 0.5 m contour interval bathymetric map (Wellner et al 2005). A Landsat 7 (ETM+) image was used to study the Lena Delta (spatial resolution of 30 m).

4.4.3 Mars Fans

The image of the Melas submarine fans used in this study was PSP_0007667_1700 taken by the HiRISE (High Resolution Imaging Science Experiment) camera onboard the

Mars Reconnaissance Orbiter. The image is in the visible spectral range, was acquired at ~3 pm local Mars time, and has a pixel size of 30 cm.

A Mars Global Surveyor Mars Orbiter Camera narrow angle mosaic of the Eberswalde delta was used to map the channels on the delta. The mosaic has a resolution of 1.5 m/pixel and was created by Malin Space Science Systems (M. C. Malin, et al., Distributary Fan Near Holden Crater, NASA's Planetary Photojournal, <http://photojournal.jpl.nasa.gov/>, PIA04869, 13 November, 2003).

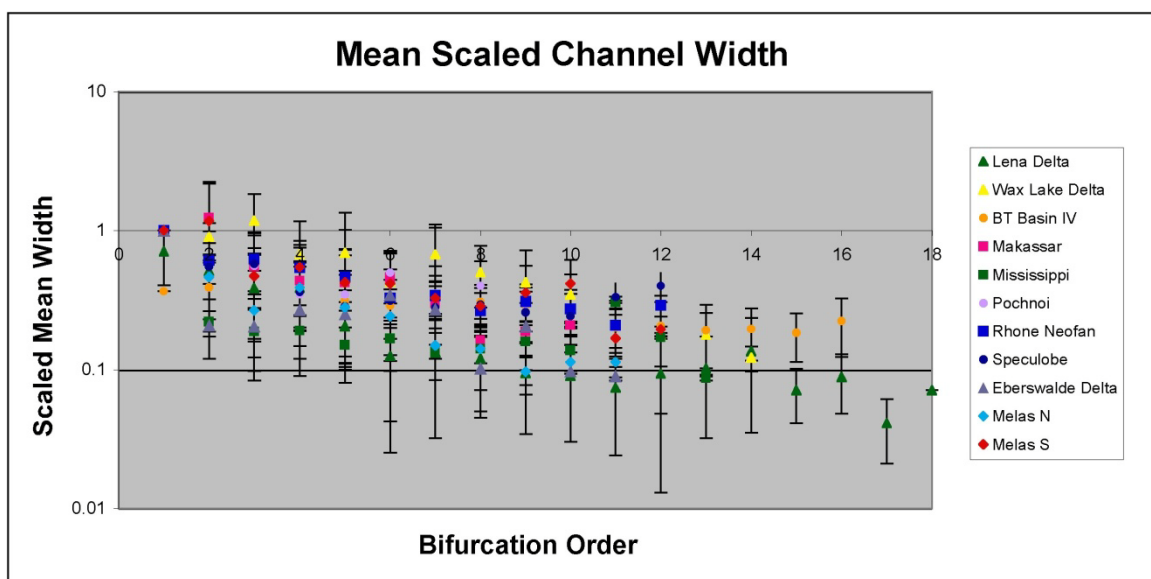


Figure 4.4 Plot of mean scaled channel width versus bifurcation order.

4.5 Methods

The properties of distributary channels were measured by hand in ArcGIS.

Channels that rejoin downstream were excluded from the analysis. We defined channels

similarly to Edmonds and Slingerland (2007) where the channel length (L) is defined as the distance between two bifurcation points along the channel centerline (Fig. 4.3). The valley length is the straight-line distance between two bifurcation points (Fig. 4.3). The channel width (W) is the average across-stream distance from water edge to water edge on the day the image was taken (Fig. 4.3).

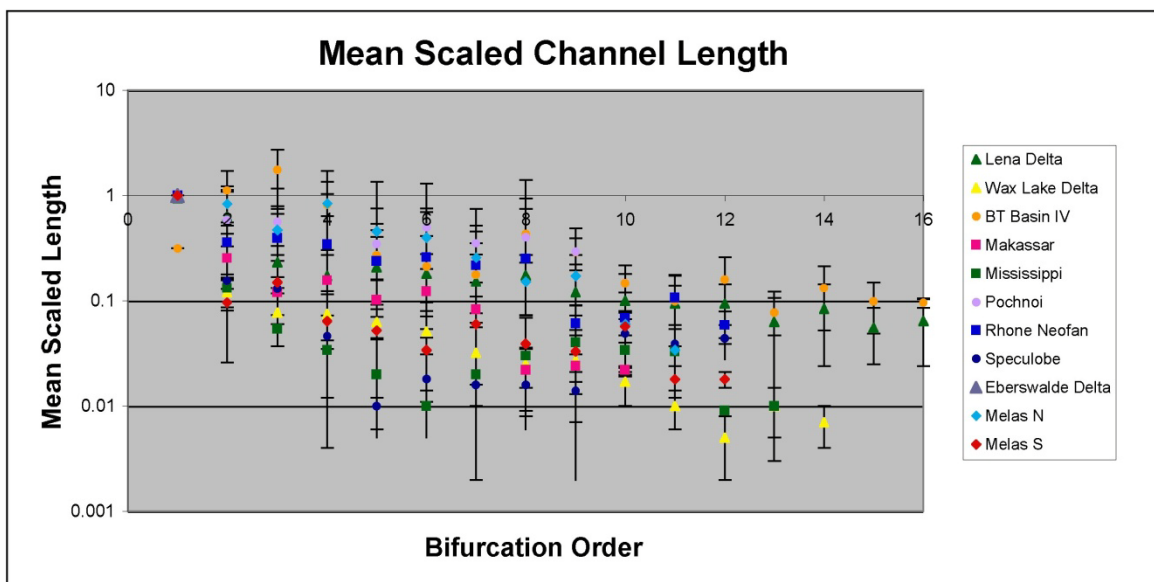


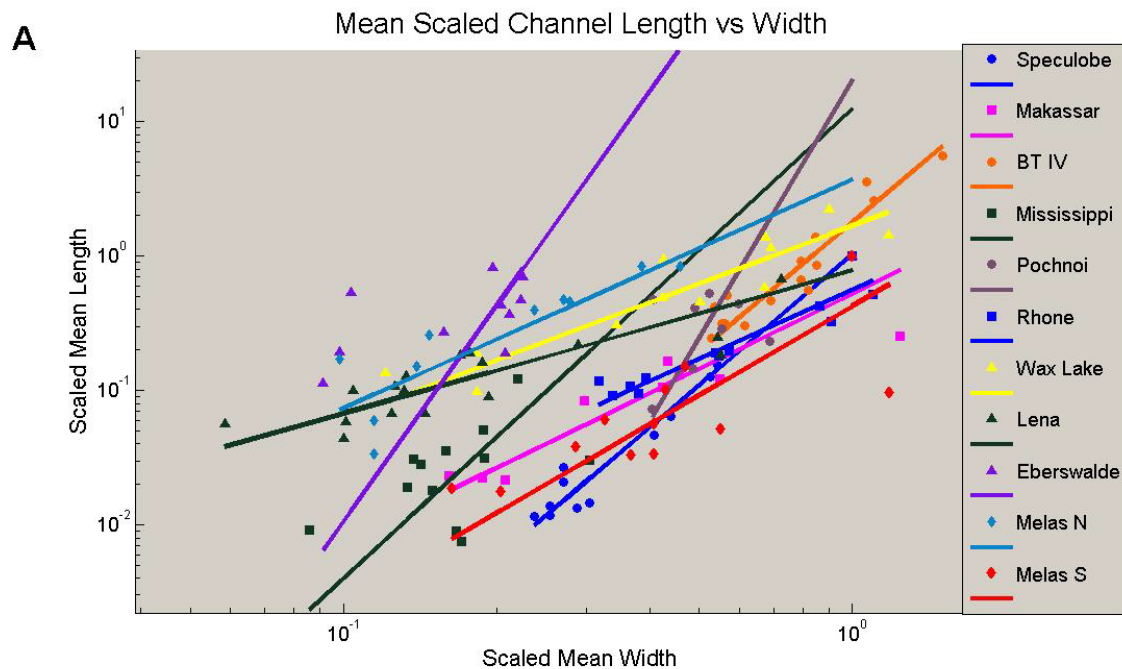
Figure 4.5 Plot of mean scaled channel length versus bifurcation order.

The mean channel widths and lengths reported are the average measurements for all channels of a particular order on a fan. The error bars in figures 4.5 and 4.7-4.8 and the uncertainties in Table 4.2 are the standard deviations of the population of channel measurements for each order. The standard deviations are fairly large due to the large range of variability in each of the parameters that were measured. The smallest channel

observed on a particular fan is limited by the resolution of the image used for analysis. The standard deviations reported for the fitted parameters n and a in Figure 4.6 were calculated using a monte-carlo analysis with 1000 iterations.

The branching angle was measured in two different ways. In the first method, after each bifurcation point the angle that a channel veers off from the straight-line path of the trunk channel is measured (A1 in Fig. 4.3). The second method measures the angle between the two channels after a bifurcation (A2 Fig. 4.3). The lines used to measure the branching angles after the split are defined by an approximation of a straight line to the centerline over about three channel diameters as measured before the channel split. The channel gradient was calculated by dividing the difference in bed elevation between the beginning and end of a channel by the channel length, since densely-spaced bathymetric data were not available. The sinuosity was calculated by dividing the channel length by the valley length. Therefore, a sinuosity of 1 is a straight channel, and a sinuosity greater than 1 is sinuous.

The goal of this study was to compare channel systems on many different fans. To this end, we sought to remove the issue of scale when looking at many different sized systems. We accomplished this by comparing only non-dimensional parameters, such as sinuosity and branching angle, and scaling other parameters to make them non-dimensional. We divided the channel width by the width of the main river or submarine channel before it has split once (defined as a first order channel) and channel length by the length of the first order channel to make these parameters non-dimensional.



B

Fan	n	a
Lena	1.1±0.1	-0.2±0.2
Wax Lake	1.4 ±0.2	0.5±0.2
Eberswalde	1.5±0.8	1.6±1
Melas N	1.7±0.4	1.3±0.6
Rhone	1.7±0.3	-0.6±0.2
Makassar	1.8±0.3	0.7±0.5
Melas S	2.2±0.6	-0.8±0.7
BT Basin IV	3.2±0.2	0.58±0.07
Speculobe	3.2±0.1	0.03±0.07
Mississippi	3.7±0.7	2.8±1
Pochnoi	7.0±1	3.3±1

Figure 4.6. A.) Log-log plot of power law fits ($L=aW^n$) to mean scaled channel length (L) versus width data (W). B.) The fitted values for n and a are shown for each fan along with the standard deviations of the fitted parameters.

Fan	Order	N	Mean Channel Width (km)	Mean Channel Length (km)	Mean Channel Gradient (m/km)	Mean Channel Sinuosity

Bering	1	4	5.402±3	89.17±87	-	1.03±0.04
	2	11	2.196±1	41.985±53	-	1.03±0.05
	3	14	3.232±2	39.396±25	-	1.07±0.09
	4	15	2.823±2	46.725±33	-	1.04±0.06
	5	12	2.644±2	36.552±26	-	1.01±0.01
	6	7	3.71±2	20.769±21	-	1.04±0.04
	7	11	2.617±1	13.062±22	-	1.04±0.08
	8	6	2.987±1	25.711±29	-	1.00±0.01
	9	4	2.182±0.5	6.464±3	-	1.01±0.02
Brazos-Trinity	1	1	0.155±0.04	0.717±0.04	-	1.09±0.01
Basin IV	2	3	0.165±0.07	2.543±1	-	1.05±0.02
	3	6	0.233±0.1	3.970±2	-	1.18±0.03
	4	6	0.171±0.07	1.855±2	-	1.05±0.03
	5	13	0.132±0.07	0.613±0.6	-	1.02±0.03
	6	14	0.123±0.04	0.480±0.4	-	1.03±0.04
	7	12	0.127±0.05	0.401±0.2	-	1.01±0.01
	8	15	0.131±0.06	0.985±1	-	1.03±0.04
	9	15	0.123±0.05	0.659±0.4	-	1.02±0.04
	10	22	0.107±0.04	0.334±0.2	-	1.02±0.05
	11	23	0.086±0.04	0.226±0.1	-	1.02±0.05
	12	14	0.088±0.04	0.362±0.3	-	1.04±0.06
	13	20	0.082±0.04	0.176±0.1	-	1.01±0.04
	14	5	0.083±0.04	0.300±0.2	-	1.05±0.1
	15	6	0.087±0.04	0.224±0.1	-	1.03±0.05
	16	4	0.095±0.05	0.217±0.04	-	1.04±0.07
	Makassar	1	3	3.189±0.1	54.857±3	1.658±0.02

	2	7	3.961±3.2	13.978±3	0.845±0.1	1.01±0.01
	3	12	1.753±1.4	6.709±2	0.746±0.2	1.03±0.03
	4	15	1.385±1	9.012±9	0.635±0.5	1.03±0.04
	5	14	1.349±1	5.757±3	0.568±0.3	1.02±0.03
	6	14	1.458±0.8	7.129±4	0.481±0.3	1.03±0.03
	7	10	0.947±0.8	4.582±3	0.496±0.3	1.02±0.02
	8	7	0.514±0.4	1.263±1	0.551±0.2	1.00±0.01
	9	4	0.598±0.4	1.237±0.4	0.739±0.3	1.00±0.01
	10	2	0.663±0.1	1.183±0.1	0.602±0.3	1.00±0.01
Mississippi	1	1	0.845±0.09	96.261±0.09	-	1.14±0.02
	2	7	0.186±0.1	11.838±5	-	1.06±0.03
	3	14	0.159±0.09	4.852±5	-	1.07±0.08
	4	22	0.160±0.09	2.994±3	-	1.06±0.08
	5	18	0.126±0.09	1.737±1	-	1.04±0.04
	6	12	0.141±0.09	0.873±0.4	-	1.02±0.03
	7	6	0.113±0.09	1.818±1	-	1.04±0.03
	8	6	0.120±0.09	2.724±4	-	1.03±0.04
	9	5	0.134±0.09	3.442±4	-	1.02±0.02
	10	2	0.116±0.09	2.944±2	-	1.02±0.02
	11	2	0.257±0.09	2.912±1	-	1.05±0.05
	12	2	0.144±0.09	0.727±0.1	-	1±0.02
	13	2	0.073±0.09	0.874±0.1	-	1±0.02
Rhone Neofan	1	2	0.145±0.04	3.300±0.3	-	1.06±0.02
	2	6	0.132±0.1	1.079±0.3	-	1.06±0.04
	3	8	0.159±0.1	1.696±2	-	1.03±0.03
	4	10	0.125±0.06	1.399±1	-	1.03±0.04

	5	17	0.083±0.04	0.647±0.5	-	1.04±0.04
	6	18	0.079±0.04	0.600±0.3	-	1.05±0.07
	7	14	0.078±0.04	0.631±0.4	-	1.05±0.05
	8	14	0.057±0.04	0.409±0.4	-	1.06±0.1
	9	12	0.055±0.04	0.313±0.2	-	1.06±0.08
	10	8	0.053±0.04	0.354±0.2	-	1.07±0.09
	11	7	0.046±0.04	0.386±0.2	-	1.02±0.03
	12	4	0.049±0.04	0.301±0.09	-	1.08±0.03
Speculobe	1	1	0.059±0.005	9.7±0.005	19.998±0.3	1.22±0.02
	2	2	0.032±0.005	1.504±0.8	8.749±0.3	1.06±0.02
	3	6	0.031±0.05	1.22±0.9	4.937±4.2	1.16±0.1
	4	9	0.026±0.008	0.622±0.6	3.219±4.8	1.07±0.05
	5	13	0.024±0.01	0.447±0.5	8.26±3.5	1.06±0.05
	6	19	0.016±0.006	0.201±0.1	5.338±4.7	1.05±0.05
	7	26	0.017±0.007	0.129±0.09	5.275±3.9	1.02±0.03
	8	27	0.015±0.005	0.115±0.09	3.807±4.4	1.02±0.03
	9	22	0.015±0.005	0.135±0.1	3.502±2.9	1.02±0.04
	10	10	0.014±0.005	0.112±0.06	6.776±4.7	1.02±0.03
	11	4	0.016±0.005	0.261±0.09	6.637±3.7	1.01±0.02
	12	2	0.018±0.008	0.142±0.02	9.697±1.9	1.00±0.02
Melas N	1	1	0.122±0.0008	0.417±0.0008	-	1.01±0.01
	2	3	0.056±0.03	0.347±0.2	-	0.032±0.04
	3	6	0.033±0.02	0.196±0.08	-	1.01±0.01
	4	5	0.047±0.03	0.349±0.09	-	1.01±0.006
	5	8	0.034±0.02	0.191±0.1	-	1.01±0.02
	6	15	0.029±0.03	0.165±0.1	-	1.04±0.06

	7	15	0.018±0.009	0.107±0.09	-	1.02±0.02
	8	14	0.017±0.009	0.063±0.03	-	1.03±0.07
	9	6	0.012±0.004	0.072±0.04	-	1.00±0.01
	10	4	0.014±0.003	0.025±0.008	-	1.03±0.06
	11	4	0.014±0.004	0.014±0.006	-	1.00±0.01
Melas S	1	1	0.049±0.0008	1.976±0.0008	-	1.04±0.01
	2	3	0.058±0.04	0.190±0.1	-	1.00±0.01
	3	6	0.023±0.01	0.297±0.2	-	1.06±0.04
	4	10	0.027±0.01	0.102±0.2	-	1.01±0.01
	5	14	0.021±0.01	0.201±0.2	-	1.02±0.03
	6	15	0.020±0.01	0.067±0.05	-	1.01±0.02
	7	24	0.016±0.007	0.119±0.1	-	1.03±0.04
	8	11	0.014±0.005	0.076±0.05	-	1.01±0.01
	9	2	0.018±0.009	0.066±0.04	-	1.01±0.01
	10	3	0.020±0.01	0.112±0.02	-	1.01±0.02
	11	4	0.008±0.004	0.037±0.01	-	1.01±0.02
	12	2	0.010±0.0008	0.035±0.005	-	1.01±0.01
Wax Lake Delta	1	1	0.355±0.09	1.399±0.09	0.357±0	1.00±0.01
	2	2	0.320±0.09	3.110±1.1	0.125±0.1	1.01±0.01
	3	5	0.417±0.2	1.993±1.1	0.319±0.2	1.00±0.01
	4	8	0.240±0.2	1.938±1.1	0.273±0.2	1.04±0.07
	5	7	0.245±0.1	1.630±0.6	0.236±0.2	1.02±0.03
	6	10	0.151±0.09	1.327±0.6	0.065±1	1.09±0.2
	7	8	0.239±0.2	0.826±0.6	0.412±0.7	1.03±0.05
	8	8	0.178±0.1	0.645±0.3	0.075±0.06	1.01±0.03
	9	16	0.150±0.1	0.685±0.4	0.552±0.5	1.04±0.05

	10	6	0.122±0.09	0.434±0.2	0.801±0.1.2	1.11±0.2
	11	4	0.074±0.09	0.255±0.1	0.057±0.08	1.10±0.1
	12	6	0.065±0.09	0.137±0.09	0.064±0.09	1.12±0.5
	13	6	0.065±0.09	0.268±0.1	0.556±1.1	1.05±0.05
	14	4	0.043±0.09	0.190±0.09	0.063±0.07	1.07±0.08
Lena Delta	1	2	4±2	66±40	-	1.07±0.002
	2	4	3.0±0.7	44±30	-	1.13±0.1
	3	6	2±2	16±8	-	1.07±0.06
	4	12	2±2	12±9	-	1.1±0.1
	5	20	1.2±0.6	14±10	-	1.11±0.2
	6	34	0.7±0.6	13±8	-	1.14±0.2
	7	40	0.8±0.6	11±11	-	1.1±0.2
	8	44	0.7±0.4	12±9	-	1.16±0.2
	9	43	0.6±0.4	9±7	-	1.12±0.2
	10	36	0.5±0.4	7±6	-	1.07±0.07
	11	42	0.4±0.3	7±5	-	1.06±0.06
	12	26	0.5±0.5	7±4	-	1.09±0.08
	13	26	0.6±0.4	4±4	-	1.03±0.06
	14	18	0.8±0.6	6±4	-	1.06±0.05
	15	12	0.4±0.2	4±2	-	1.05±0.05
	16	6	0.5±0.2	4±3	-	1.09±0.05
	17	4	0.24±0.09	4±1	-	1.04±0.03
	18	2	0.4±0.08	2.8±0.2	-	1.07±0.02
Eberswalde	1	3	0.52±0.2	1.8±0.6	-	1±0.03
Delta	2	14	0.10±0.1	1.6±0.7	-	1.15±0.3
	3	26	0.12±0.1	1.5±1	-	1.11±0.1

	4	33	0.12±0.1	1.0±1	-	1.13±0.2
	5	33	0.11±0.5	0.87±1=0.7	-	1.09±0.2
	6	18	0.11±0.06	0.73±0.5	-	1.07±0.1
	7	5	0.08±0.7	0.50±0.2	-	1.03±0.03
	8	5	0.05±0.5	1.1±0.5	-	1.09±0.05
	9	7	0.11±0.1	0.36±0.4	-	1.02±0.03
	10	2	0.05±0.01	0.37±0.3	-	1.05±0.05
	11	2	0.05±0.01	0.21±0.03	-	1.07±0.03

Table 4.2 Number of channels in each bifurcation order, mean channel width, mean channel length, mean gradient and mean channel sinuosity. We did not have bathymetry data for fans with no channel gradient reported.

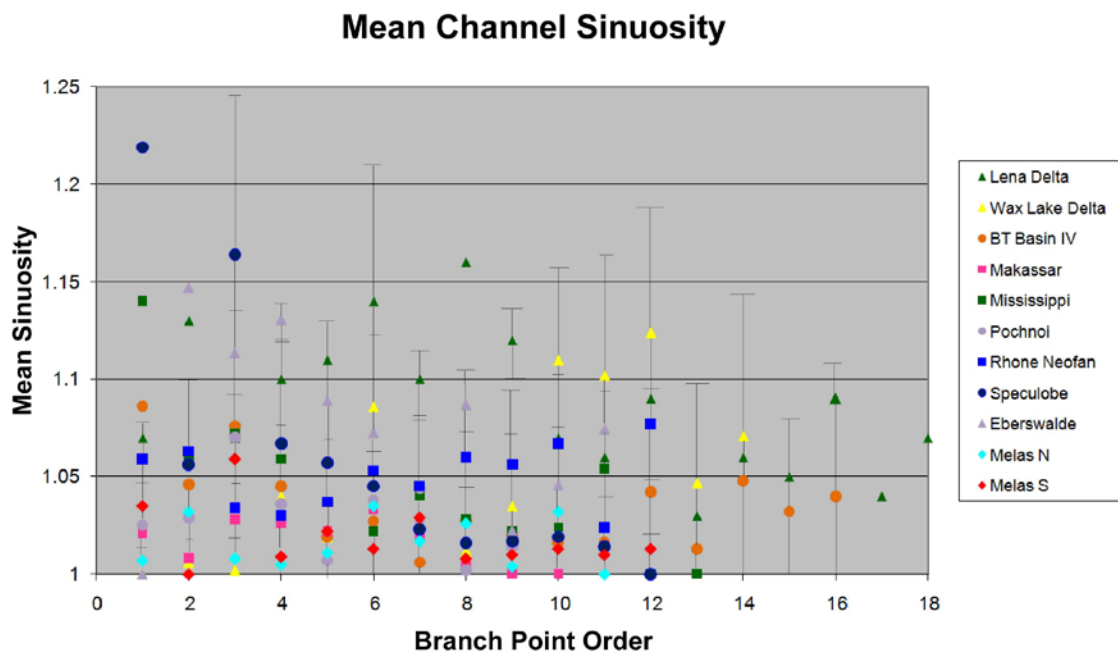


Figure 4.7 Plot of mean channel sinuosity versus bifurcation order.

4.6 Results

The channels were defined by the method described in section 4.3, and Table 4.2 shows the number of channels mapped in each system, the mean channel width, channel length, gradient, and sinuosity. A plot of the mean channel width for each order of channel is shown in Fig.4.4. This figure shows that the mean channel width generally decreases as the order increases, similar to the trends found by Edmonds and Slingerland (2007) for deltas, although for a few fans, the second and third order channels are wider than the main channel. The mean width tends to decrease by less than 50% with each decrease in channel order. Some channels also widen over the last few orders as seen on the Speculobe, Makassar, Brazos-Trinity-Basin IV and Melas South fans.

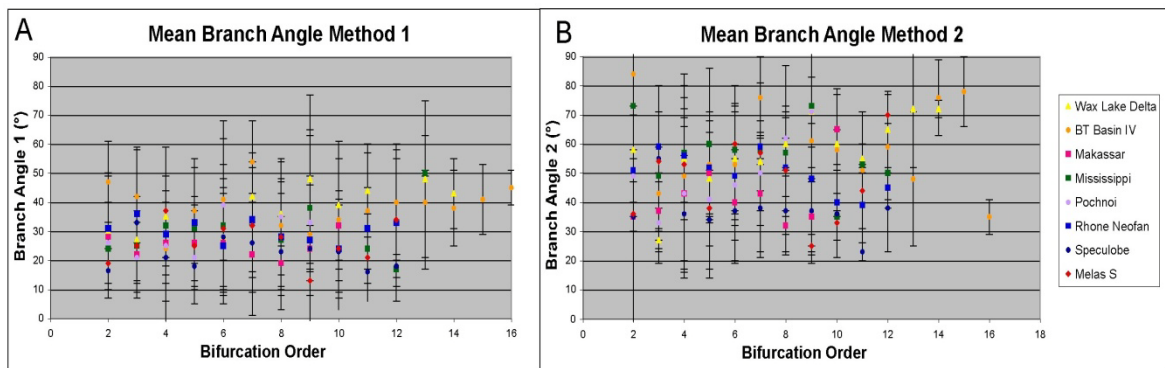


Figure 4.8 Channel branching angle versus bifurcation order. A.) Using method 1 to define branching angle. B.) Using method 2 to define branching angle.

The plot of mean scaled channel length for each order is shown in Fig. 4.5 and shows that the mean channel length decreases with increasing bifurcation order, similar to the trends found by Edmonds and Slingerland (2007) for deltas. The channel length decreases rapidly on the Makassar, Mississippi, and Melas S fans, and on the Wax Lake

Delta and then stays fairly constant. The decrease in channel length is smaller and fluctuates more widely on the Brazos-Trinity Basin IV, Melas N, Pochnoi, Rhone Neofan and Lena Delta.

Mean scaled channel length and mean scaled channel width appear to correlate. The mean channel length roughly decreases with decreasing mean channel width as shown in Fig. 4.6. The correlations of mean scaled channel width versus mean scaled channel length can be fit reasonably well with power laws as shown in Fig. 4.6a (R^2 values between 0.62-0.87). The power law fits can be represented by the equation $L=aW^n$, and the fitted values for a and n are shown in Fig. 4.6b along with the uncertainties on these parameters. The channel width versus length for the Pochnoi fan alone is not well fit by a power law. The three deltas in this study (the Lena delta ($n=1.1\pm0.1$), the Wax Lake delta ($n=1.4\pm.2$) and the Eberswalde delta ($n=1.5\pm0.8$)) have similar values for the fitted exponent n and exponents smaller than those found for the submarine fans. The exponent of the Pochnoi fan is significantly larger than the other fans ($n=7.0\pm1$), but this system was not well fit by a power law. The exponents of all the submarine fans fall within the range 1.7-3.7 which are higher those of the deltas, but with the uncertainties in these exponents, the two types of fans cannot be wholly distinguished.

The mean channel sinuosity is fairly low (<1.3) for all of the systems that were examined (Fig. 4.7). The Makassar fan has a roughly constant mean sinuosity of 1.03, whereas the Speculobe fan mean sinuosity varies between 1.05-1.23 and the Wax Lake Delta between 1.07-1.12.

The gradient (Table 4.2) has no systematic trend with channel order for the Makassar deep sea fan, the Speculobe fan or the Wax Lake Delta. The input channel has a larger gradient on the Makassar and Speculobe fans because the channel is only defined for the steeper part of the system and is not extended through the length of the entire system.

The mean branching angle for method 1 varies between 15-55° (Fig. 4.8A). There is no systematic trend in the dataset. The mean branching angle for method 2 varies between 20-85° (Fig. 4.8B). Again, there does not appear to be any systematic trend between branching angle and the order of the channel. There also does not appear to be a relation between mean branch angle and gradient.

4.7 Discussion

4.7.1 Nature of Channel Bifurcations

The decrease in channel width with increasing bifurcation order on delta distributary channels implies that the channel width is decreasing in a down-fan direction as the channels continue to bifurcate. This is not unexpected since a nonlinear decrease in channel width after channel bifurcation has been previously found in delta distributary channels and is expected by predictions of hydraulic geometry relations (Edmonds and Slingerland 2007). We found a similar trend of decreasing width with increasing bifurcation order on submarine fans. When a turbidity current is flowing through a channel and that channel splits, if both of the channel branches are active simultaneously one would expect the cross-sectional area of each of the channels after the split to be smaller than that

of the previous single channel. If the discharge of the turbidity current and the depth of the channels stay roughly constant, then the width of the channels should decrease after each split. This is observed for all of the fans examined. A decrease in channel width after channel bifurcation indicates that both branches of the channel were active simultaneously; otherwise the width after a bifurcation should be comparable to the width before the bifurcation. The method used to map the channels in this study does not distinguish between channel avulsion and channel bifurcation in most cases. Cross-sectional views were not available to determine whether the channel avulsed to a new path or simply bifurcated. In a few areas it was possible to see crosscutting relationships between channels, and in these instances, it was possible to distinguish between channel bifurcation and avulsion. However, the result that channel width decreases downfan does not necessarily imply that an original channel and a channel that formed during an avulsion were active simultaneously.

Studies of the channels on upper and middle submarine fans came to similar conclusions. Flood and Damuth (1987) found that both channel width and depth decrease down the submarine fan, and hence there was a decrease in the cross-sectional area of the channels down fan. They suggested that this implied a down-fan decrease in the maximum thickness and total volume of the turbidity currents that flow down the channels. Since the finer material in the turbidity current can spill over the edge of the channel more easily, they suggest that the remaining flows should become coarser and better sorted down-fan.

For the Speculobe, Makassar, Brazos-Trinity-Basin IV and Melas South fans, there appears to be a slight increase in channel width near the termination of the channel system (at the largest bifurcation orders). The slight increase in channel width at their distal limits could be due to shallowing of the channels and spreading of the flow. This is supported by sub-bottom profiles that transect the channels on the Makassar fan and show that the depth of the channels is less near the distal limit (Orange et al. 2006). These profiles show that channels near the distal limits of the fan have very little topographic signature.

Our study found that channel length decreases downfan with increasing bifurcation order on the three deltas examined. This is not unexpected since Edmonds and Slingerland (2007) also found that channel length decreases non-linearly with channel bifurcations and suggested that the channel length between bifurcations is proportional to the jet momentum flux and depends on the depth of the initial channel. Their modeling suggests that the distance between bifurcations is not a function of simple grain settling since this process does not account for mouth bar progradation observed in the field.

Channel length also decreases downfan on the submarine fans examined in this study. On several of the submarine fans (Rhone Neofan, Pochnoi, BT Basin IV and Melas North), the channel length is variable but continues to decrease down fan similar to the trend observed on deltas. This could imply a variable but increasing rate of sediment deposition from the turbidity current, which results in the variable but decreasing channel lengths seen on these submarine fans. On the other submarine fans (Mississippi, Melas South, Makassar, and Speculobe), the decrease in mean channel length with increasing

bifurcation order shows that the main trunk channel of submarine fans tends to be fairly long, and then the channel reaches a point where it begins to bifurcate after a short distance. After this point, the mean channel length stays roughly constant. In the submarine case, a channel will bifurcate when a lobe has built up high enough to divert the flow. The behavior of turbidity currents around obstructing topography depends on several factors including the velocity of the current, the obstacle height, the current density and the density stratification within the current (Kneller and Buckee 2000). Lane-Serff et al. (1995) found that part of the head of turbidity currents can surmount obstacles up to four or five times the ratio of the obstacle height to current body thickness or less than 1.5 times the flow thickness (Muck and Underwood 1990). This could imply that in the submarine fans where the length of the main channel is long and then subsequent channels rapidly decreases to a constant length, the turbidity current does not lose much material at first, since it takes a significant distance to build up a lobe high enough to divert the flow. Then once it has reached this state, the current should lose material at a roughly constant, but faster rate than previously, so that the subsequent channels bifurcate after a roughly equivalent distance. The trends in bifurcation length do not seem to correlate with the size of the fan, the dominant grain size present on the fan, or the water depth of the fan.

The branching angle of the channels appears to be highly variable. These angles do not seem to be related to the order of the channel (i.e. position on the fan) or to the slope of the fan surface. The branching angle varies over a wide range and may depend on a complicated set of factors that we are unable to separate. The method of measuring branching angles that Olariu and Bhattacharya (2006) used to differentiate among different

delta types was not meaningful when applied to submarine fans. No trends or patterns could be recognized in these branching angles.

4.7.2 Mean Channel Length versus Width Trends

The mean channel length versus width on the various fans follows a power law trend as discussed above. How quickly or slowly the channel widths decrease for a given decrease in channel length (i.e. in a steep trend the channel length falls off faster for a given decrease in channel width), does not appear to correlate with the dominant grain size present on the fan or the water depth. To first order both deltas and submarine fans show a similar range of length versus width trends, but the fitted exponent n for deltas is slightly less than those found on submarine fans. Taking into account the uncertainties on the values, the two types of fans overlap in their range of n . Large values of n ($n > 2.3$) are only found on submarine fans; however, the sample size of deltas investigated in this study is small and examination of additional deltas may find deltas with larger n .

The fact that the length versus width distributions of submarine fans and deltas overlap may be due to the amount of error in the data obscuring the differences in processes that lead to channel formation in each type of fan. Or, submarine fans and deltas might have similar advection length scales which could lead to overlapping length versus width trends.

4.7.3 Sinuosity

Unlike on upper and middle submarine fans, the mean channel sinuosity on lower submarine fans is quite low. In this study the mean sinuosity on lower submarine fans ranges from 1.0-1.23, but is typically less than 1.05. The sinuosity of the channels on the upper and middle Amazon submarine fan ranges from 1.05-2.6 (Flood and Damuth 1987). Clark et al. (1992) measured the sinuosity of channels on 16 different submarine fans and found values as high as 3 with average values appearing closer to 1.3-1.5. Thus, it appears that channels on the lower parts of submarine fans are much less sinuous than those farther up fan.

Laboratory experiments on sediment deposition by turbidity currents in sinuous channels show that sediment is preferentially deposited on the outer bends of channels, leading to an asymmetric channel cross-section and a relative straightening of the channel (Straub et al. 2008). This suggests that perhaps continued deposition in outer channel bends leads to straightening of the channels and the much lower sinuosities observed on lower submarine fans.

4.7.4 Reservoir Model Applications

The mean and range of values found for measurements of channel width and length as shown in Table 4.2 can be used to constrain the dimensions of sand bodies in static reservoir models of submarine channels and deltas. Our determination of stochastic branching angles indicates such branching angles can be used realistically in reservoir models, instead of just being assumed for simplicity's sake. Most reservoir models use the same value for sinuosity on lower submarine fans as was used for the upper fan, but our

results show that the channel sinuosity is lower on distal submarine fans and should be modeled with a lower value in reservoir models. The combination of these results helps to constrain the lateral connectivity of sand bodies that may serve as reservoirs.

4.7.5 Effects of Martian Gravity

Another potential application of channel bifurcation mapping is to help interpret depositional fans observed on other planets. If a depositional fan is observed on Mars, whether the fan formed subaqueously or at the air-water interface has different implications for the environmental conditions present when the fan formed. The observation of a submarine fan on Mars would imply a relatively deep and perhaps long-lived body of water whereas a delta could form in a much shallower body of water. Since one of the goals of Mars exploration is to understand the past extent of liquid water at the surface, this distinction has become relevant with the recent observation of a potential ancient submarine fan (chapter 3 of this thesis). If the channel patterns on submarine fans and deltas were distinct, then this observation would provide an important criterion to interpret depositional fans observed on other planets.

The Melas North and South fans on Mars are small fans, and the slope of their power law fits falls within the lower part of the range of values found on the larger terrestrial submarine fans. This means the Melas fans have channels that are slightly longer for a given width than the terrestrial submarine fans. This could be due to similar bifurcation behavior, but because Mars has lower gravity ($g=3.7 \text{ m/s}^2$) it could cause the sediment to be carried farther by a given flow on Mars than a similar flow on Earth. The

advection distance for a particle traveling in a turbidity current is given by

$$L = \frac{uh_s}{\omega_s} \quad (1)$$

where ω_s is the settling velocity, u is the flow speed and h_s is the height of the sediment particle above the bed (see Fig. 4.9). The flow speed of a turbidity current is given by

$$u = \left(\frac{\rho g H S}{C_f} \right)^{\frac{1}{2}} \quad (2)$$

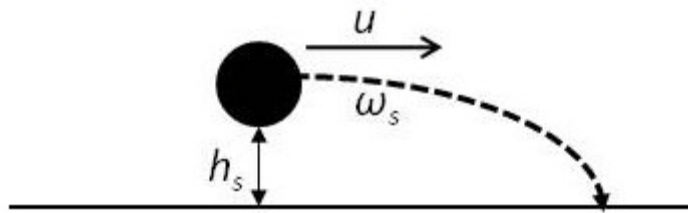


Figure 4.9 Diagram illustrating the settling of a particle at a height h_s above the bed in a flow traveling at a flow speed u .

where ρ is the density, g is the acceleration due to gravity, H is the flow depth, S is the slope, and C_f is the form drag coefficient. The settling velocity for small grains (< 1 mm) is given by

$$\omega_s = \frac{1}{18} \frac{RgD^2}{\nu} \quad (3)$$

where R is the submerged specific density of grains, D is the grain diameter, and ν is the kinematic viscosity. Substituting equations (2) and (3) into equation (1) yields $L \propto g^{-1/2}$.

Thus, for the same current, the ratio of the advection length of a particle on Mars to the

advection length of a particle on earth is $\frac{L_{Mars}}{L_{Earth}} \propto \frac{g_{Mars}^{-1/2}}{g_{Earth}^{-1/2}}$ which gives $L_{Mars} = 1.63 L_{Earth}$.

Our observation of longer channels on Mars agrees with the predictions of a longer advection length scale on Mars due to the lower gravity.

4.8 Conclusions

After mapping the terminal channel systems on six terrestrial submarine fans, two Martian submarine fans, two terrestrial deltas and one Martian delta, some trends are apparent. Mean channel width and length decrease nonlinearly down fan. The channel sinuosity on lower submarine fans is much lower than further up fan. Channel branching angles appear to be stochastic and do not provide a meaningful measure to discriminate between fans. The trends of mean channel length versus mean channel width follow power laws. The exponent in the fits of channel length versus channel width is slightly smaller for deltas than for submarine fans, but the range of values of n overlaps for the two types of fans. Channel lengths fall off slightly more slowly for a given decrease in channel width on Mars which may be the result of a longer advection length scale due to the lower gravity.

This study has allowed us to characterize the variability in channel size and bifurcation pattern present in channel systems at the distal limits of submarine fans. This information will be useful in constraining channel properties in static reservoir models, e.g. the mean and range of values typical for channel dimensions, sinuosity, and branching angles.